Brucella abortus promotes a fibrotic phenotype in hepatic stellate cells with concomitant autophagy pathway activation

Paula Constanza Arriola Benitez[1], Ayelén Ivana Pesce Viglietti[1], Claudia Karina Herrmann[2], Vida A. Dennis[3], Diego José Comerci[2], Guillermo Hernán Giambartolomei[1] and María Victoria Delpino[1].

Instituto de Inmunología, Genética y Metabolismo (INIGEM). CONICET. Universidad de Buenos Aires. Buenos Aires, Argentina[1]. Instituto de Investigaciones Biotecnológicas Dr. Rodolfo A. Ugalde (IIB-INTECH) CONICET, Universidad Nacional de San Martín, Buenos Aires, Argentina[2]. Center for NanoBiotechnology Research, Alabama State University, Montgomery, AL 36104[3]

Running title: *B. abortus induces autophagy in hepatic stellate cells*

Corresponding author:

M. Victoria Delpino, PhD.

INIGEM, Instituto de Inmunología, Genética y Metabolismo. Hospital de Clínicas "José de San Martín". Facultad de Medicina, Universidad de Buenos Aires, Córdoba 2351 piso 3 sala 4, 1120. Buenos Aires, Argentina.

Phone: 54-11-5950-8755.

Fax: 54-11-5950-8758.

E-mail: mdelpino@ffyb.uba.ar

ABSTRACT

The liver is frequently affected in patients with active brucellosis. The present study demonstrates that *B. abortus* infection induces the activation of the autophagic pathway in hepatic stellate cells to create a microenvironment that promote a profibrogenic phenotype through the induction of transforming growth factor-β1 (TGF-β1), collagen deposition and inhibition of matrix metalloproteinase-9 (MMP-9) secretion. Autophagy was revealed by up-regulation of the LC3II/ LC3I ratio and beclin-1 expression as well as inhibition of p62 expression in infected cells. The above findings were dependent on the type IV secretion system (VirB) and the secreted BPE005 protein; which were partially corroborated using the pharmacological inhibitors wortmannin - a PI3-kinase inhibitor - and leupeptin plus E64 (inhibitors of lysosomal proteases). Activation of the autophagic pathway in hepatic stellate cells during *Brucella* infection could have an important contribution in attenuating inflammatory hepatic injury by inducing fibrosis. However, with time, *B. abortus* infection induced beclin-1 cleavage with concomitant cleavage of caspase-3 indicating the onset of apoptosis of LX-2 cells, as was confirmed by the TUNEL assay and Hoechst staining. These results demonstrate that the crosstalk of LX-2 cells and *B. abortus* induces autophagy and fibrosis with concomitant apoptosis of LX-2 cells, which may explain some potential mechanisms of liver damage observed in human brucellosis.

INTRODUCTION

Human brucellosis, a zoonotic infection caused by *Brucella* species, is an inflammatory disease with inflammation being present both in the acute and chronic phases of the disease and in virtually all of the organs affected (1-3). The liver is frequently affected in patients with active brucellosis and although numerous studies have focused on brucellar liver histopathology (1, 2, 4-6), the pathogenic mechanisms of *Brucella* liver disease have not been completely investigated at the molecular and cellular levels.

Liver fibrosis is a wound-healing response to chronic hepatic injury (7, 8). An early event in the development of liver fibrosis is the activation of hepatic stellate cells (HSCs), the major cell type responsible for increased synthesis of extracellular matrix proteins (9). Increased transforming growth factor (TGF)-β1 levels are also observed in the damaged liver and this has a close correlation with fibrogenic changes in HSCs and liver tissue (10-12).

It has been demonstrated that autophagy is involved in the fibrotic response to chronic hepatic injury caused by alcohol abuse, hepatitis virus infection and nonalcoholic steatohepatitis (13). Autophagy is a catabolic intracellular pathway, targeting defective or excessive organelles to the lysosomes for degradation into amino acids, free fatty acids or other small molecules used for material recycling or energy harvest (14). Autophagy, usually stimulated by energy restriction, stress or inflammation, is regarded as a survival mechanism that plays a critical role in maintaining cellular homeostasis, which is involved in many human disorders including fibrotic disease (15). During fibrosis, autophagy is mostly a cell survival mechanism that attenuates hepatic inflammatory injury and ultimately induces liver fibrosis (14).

Previously, we have demonstrated that upon infection of hepatic stellate cells, *B. abortus* triggers a profibrogenic response characterized by the inhibition of MMP-9 secretion, collagen deposition and TGF-β1 secretion. This involves a functional T4SS and its effector protein BPE005 of *B. abortus*. The TGF-β1 pathway is a classical signaling pathway activated in liver fibrosis that also induces autophagy (16). This suggests that autophagy could participate in fibrosis during *Brucella* infection in a way that depends on TGF-β expression. Thus, we hypothesized that *Brucella* infection might create a microenvironment that promotes a profibrogenic phenotype and induces the activation of the autophagic pathway, which could have an important contribution in attenuating hepatic injury in the liver of patients with *Brucella* infection.

MATERIALS AND METHODS

Bacterial Culture

Brucella abortus S2308, its isogenic *virB10* polar, *bpe005* mutants and complemented strain of the *bpe005* mutant (17) were grown overnight in 10 ml of tryptic soy broth (Merck, Buenos Aires, Argentina) with constant agitation at 37°C. Bacteria were harvested and the inocula were prepared as described previously (18). All live *Brucella* experiments were performed in biosafety level 3 facilities located at the Instituto de Investigaciones Biomédicas en Retrovirus y SIDA (Buenos Aires, Argentina).

Cell Culture

LX-2 cell line, a spontaneously immortalized human hepatic stellate cell line, was a gift from Dr. Scott L. Friedman (Mount Sinai School of Medicine, New York, NY). LX-2 cells were maintained in Dulbecco's modified Eagle's medium (Life Technologies-Invitrogen, Carlsbad, CA) and supplemented with 2 mmol/L of L-glutamine, 100 U/mL of penicillin, 100 µg/mL of streptomycin, and 5% (v/v) fetal bovine serum (Gibco-Invitrogen, Carlsbad, CA). Cells were seeded at 5 x 10^4 cells/well in 24-well plates and were cultured at 37°C with 5% CO_2.

Cellular Infection

LX-2 cells were infected with either *B. abortus*, its isogenic *virB10*, *bpe005* mutants or the complemented *bpe005* mutant strain at different multiplicities of infection (MOI). After the bacterial suspension was dispensed, the plates were

centrifuged for 10 min at 2000 rpm and then incubated for 2 h at 37°C in a 5% CO_2 atmosphere. Infected cells were extensively washed with Dulbecco's modified Eagle's medium to remove extracellular bacteria and then incubated in medium supplemented with 100 µg/ml of gentamicin and 50 µg/ml of streptomycin to kill extracellular bacteria. LX-2 cells were harvested at different times of infection depending on the specific experiment to determine autophagy, apoptosis and fibrosis markers.

Western blotting

Infected LX-2 cells were lysed in ice-cold lysis buffer consisting of 1% Triton X-100 in 150 mM NaCl, 25 mM Tris-HCl (TBS) pH 7.4, and a protease inhibitor cocktail (Sigma-Aldrich). Lysates were incubated on ice for 10 min and cleared by centrifugation at 13,000g for 10 min. Protein concentrations were determined by the bicinchoninic acid method (Pierce, Rockford, IL, USA) using bovine serum albumin as standard. Equal amounts of proteins were loaded onto electrophoresis gels and after separation; proteins were transferred to a nitrocellulose membrane (GE Healthcare, Little Chalfont, UK) and blocked for 1 h with 5% milk protein-0.05% Tween 20. After blocking, membranes were incubated with rabbit anti-LC3B (Cell Signaling Technology, Danvers, MA), goat anti-BECN-1 (Santa Cruz Biotechnology) or rabbit anti-p62/ SQSTM1 (R&D Systems) overnight at 4°C, followed by washing and then incubated with a 1:1,000 dilution of peroxidase-conjugated secondary antibody (Santa Cruz Biotechnology) for 1 h. Protein bands were visualized on Hyperfilm ECL (GE Healthcare) by chemiluminescence. Equal loading was confirmed by Ponceau S, acid red staining and by incubation of the blots with an anti-β-actin antibody (clone C4; Santa Cruz Biotechnology).

Immunofluorescence

LX-2 cells were infected with *B. abortus* and after 24 or 48 h postinfection were fixed in 4% paraformaldehyde for 10 min at room temperature, permeabilized with 0.3% Triton X-100 (Roche Diagnostics GmbH, Mannheim, Germany) for 10 min and blocked with PBS containing 1% bovine serum albumin (BSA) for 1 h. Infected cells were stained with rabbit anti- LC3B (Cell Signaling Technology, Danvers, MA), goat anti-BECN-1 (Santa Cruz Biotechnology) or rabbit anti-cleaved caspase-3 (Cell signaling Technology) diluted in 0.1% PBS-Tween-20 overnight at 4°C. Then, cells were incubated with Alexa Fluor 488 anti-rabbit (Jackson ImmunoResearch Laboratories) or Alexa Fluor 488 anti-goat (Molecular probes, Life Technologies) diluted in 0.1% PBS-Tween for 4 h at room temperature. DAPI was used for nuclear staining and cells were stained for 30 min at room temperature. After washing in PBS, cells were mounted and then were analyzed by fluorescence microscopy.

Apoptosis Assays

LX-2 cells were infected with *B. abortus* or its isogenic *virB10* polar mutant and were harvested 48 h later. Cells were washed, and the percentage of apoptotic cells was assessed by fluorescence microscopy after they were labeled by the terminal deoxynucleotidyl transferase-mediated dUTP-biotin nick end labeling (TUNEL) assay or by staining with the Hoechst 33342 dye. As a positive control, cells were treated with 200 µM hydrogen peroxide.

Inhibitors

To study the potential involvement of molecules that participate in autophagy pathways in the induction of collagen deposition, increase of TGF-β secretion and MMP-9 inhibition by *B. abortus* infection in LX-2, wortmannin or E64 plus leupeptin (19) (Sigma-Aldrich de Argentina S.A.) were added 2 hours after infection. Wortmannin was used at a concentration of 10 μM and E64 plus leupeptin were used at a concentration of 20 μM. To study the role of autophagy pathways in the induction of collagen deposition, increase of TGF-β secretion and MMP-9 inhibition by BPE005 protein, LX-2 cells were transfected with BPE005 plasmid or pCDNA3-c-myc, as a control of transfection efficiency as was previously described (17). After transfection, cells were treated with wortmannin or leupeptin plus E64, at the previously mentioned concentrations or with, bafilomycin A1 or chloroquine (19). Bafilomycin A1 (Sigma-Aldrich) was used at a concentration of 200 nM and chloroquine (Sigma-Aldrich) was used at a concentration of 50 μM.

Zymography

Gelatinase activity was assayed by the method of Hibbs et al with modifications, as described (18, 20, 21).

Assessment of Collagen Deposition by Sirius Red Staining

Collagen deposition was quantified using Sirius Red (Sigma–Aldrich), a strong anionic dye that binds strongly to collagen molecules. Sirius Red staining was performed as was described (17, 22).

Measurement of Cytokine Concentrations

188 TGF-β1 expression was determined in the culture supernatants by enzyme-
189 linked immunosorbent assay (ELISA; BD Biosciences, San Jose, CA).
190
191 **Statistical analysis**
192
193 Statistical analysis was performed with one-way analysis of variance (ANOVA),
194 followed by post hoc Tukey's test using GraphPad Prism 5.0 software. Data are
195 represented as means ± standard deviations (SD).
196

RESULTS

B. abortus infection induces LC3-II and Beclin-1 expression in LX-2 cells

It has been demonstrated that autophagy participates in HSCs activation (23). We have previously demonstrated that *B. abortus* infection induces HSCs activation leading to a profibrogenic phenotype (17, 22). To determine if *B. abortus* infection induces the activation of the autophagic pathway in HSCs, we evaluated by Western blot at 24 h post infection the expression of LC3 II, the lipidated form of LC3 I and the only known protein that specifically associates with autophagosomes (24); the autophagy regulator Beclin-1 (25); and p62, that participates in the autophagic clearance of ubiquitinated proteins (26). *B. abortus* infection induced an increase in the LC3 II/LC3 I ratio, an increase in Beclin-1 expression and the inhibition of p62 expression (Fig. 1). These results indicate that autophagy was induced by *B. abortus* in LX-2 cells.

B. abortus induction of a profibrogenic phenotype on LX-2 cells depends on PI3-kinase and lisosomal proteases

Acquisition of a fibrogenic phenotype by resident HSCs is a critical event of the liver's response to injury. Increasing evidences support the notion that autophagy participates in the pathophysiology of hepatic fibrosis (14). A key cytokine involved in fibrosis is TGF-β1 (27). We have demonstrated that *B. abortus* infection induced fibrosis *in vitro* and *in vivo* as revealed by collagen deposition and MMP-9 down-modulation in a mechanism that is dependent on TGF-β1 (22). Thus, experiments were conducted to determine whether fibrosis induced by *B. abortus* infection is dependent

on the autophagy activation. To this end, we examined markers of a fibrogenic phenotype including the secretion of TGF-β1, the deposition of collagen and the down-modulation of MMP-9 in LX-2 cells during *B. abortus* infection in the presence of wortmannin (a PI3-kinase inhibitor) and leupeptin plus E64 (inhibitors of lysosomal proteases). Both, wormannin and leupeptin plus E64 reversed *B. abortus*-induced MMP-9 down-modulation, collagen deposition and TGF-β1 secretion (Fig. 2A to C). Accordingly, when we performed the infection experiment in the presence of rapamycin, an autophagy inductor, we observed an increase of the fibrotic phenotype respect to infected but untreated cells corroborating the association between autophagy and fibrosis (Fig. 2D and E). These results indicate that autophagy could be involved in the induction of the fibrotic phenotype in *B. abortus*-infected LX-2 cells.

B. abortus induces autophagy in LX-2 cells in a VirB-dependent manner

The type IV secretion system (T4SS) VirB is vital for *Brucella* to establish an intracellular replication niche (28), and it also has been involved in the induction of inflammatory responses during infection (11, 29-31). In addition, we have previously demonstrated that the fibrotic phenotype induced by *B. abortus* in LX-2 cells is dependent on a functional T4SS (17). As such, we tested whether VirB was involved in the activation of the autophagy signaling pathway. Our results demonstrate that *B. abortus* wild type infection increased the expression of LC3 II and Beclin-1. Yet, when LX-2 cells were infected with *B. abortus virB10* mutant, LC3 II and Beclin-1 levels did not differ significantly from uninfected cells (Fig. 3). These results indicate that the activation of the autophagy signaling pathway depends on a functional T4SS.

VirB-dependent effector protein BPE005 is involved in the autophagic phenotype induced by *B. abortus* in LX-2 cells

Recently, *B. abortus*-secreted effectors have been identified to require a functional VirB system to be translocated into the host cells (31-39).

Our previous results indicated that the secreted protein BPE005 is involved in the induction of a fibrogenic phenotype in LX-2 cells, (17). Thus, we decided to determine whether BPE005 is also involved in the induction of autophagy. To this end, we evaluated if *B. abortus bpe005* mutant was able to induce the expression of LC3 II; the only protein known that specifically associates with autophagosomes. As occurred with the *B. abortus virB* mutant, when LX-2 cells were infected with *B. abortus bpe005* mutant, there was no increment in the levels of LC3 II with respect to LC3 I. In addition, the complemented *bpe005* mutant restored the ability to induce autophagy observed in the wild type strain (Fig. 4).

In addition, and taking into account that *Brucella* could use some components from autophagy pathway to establish its replicative niche (40, 41), experiments were performed to corroborate the association between autophagy and the fibrotic phenotype induced by BPE005 in LX-2 cells. To this end, LX-2 cells were transfected with a eukaryotic expression vector harboring the *bpe005* gene and the levels of MMP-9 activity, collagen deposition, and TGF-β1 secretion were determined. Expression of BPE005 protein in LX-2 cells was able to inhibit MMP-9 activity and to induce collagen deposition and TGF-β1 secretion and these phenomena were reversed when experiments were performed in the presence of wortmannin (a PI3-kinase inhibitor), and leupeptin plus E64 (inhibitors of lysosomal proteases), bafilomycin or chloroquine (two inhibitors of autophagosome-lysosome fusion) (Fig. 5).

Taken together, these results indicate that *B. abortus* induces autophagy pathway activation in a mechanism that is dependent on the presence of T4SS and its secreted protein BPE005, with concomitant fibrosis dependent on PI3-kinase, lysosomal proteases and autophagosome-lysosome fusion.

B. abortus infection induces cleavage of Beclin-1 with concomitant apoptosis

In spite of the ability of *Brucella* infection to induce a fibrotic phenotype in HSCs (17, 22), liver cirrhosis is a debatable issue in *Brucella*-infected humans (5) indicating a possible balance between fibrotic and antifibrotic factors involved during infection. Increasing HSCs death is a possible explanation for limiting liver fibrosis.

Beclin-1 is a dual regulator of both autophagy and apoptosis. When we evaluated Beclin-1 expression at 48 h post-infection our results indicated that *B. abortus* infection induces Beclin-1 cleavage (Fig. 6). Caspase-3-mediated cleavage of Beclin-1 promotes crosstalk between apoptosis and autophagy (42). Then, experiments were conducted to determine if *B. abortus* infection induces apoptosis in LX-2 cells at 48 h post-infection. To this end, LX-2 cells were infected with *B. abortus* and the presence of apoptotic cells was determined by TUNEL assay, cleaved caspase-3 expression, and Hoechst 33342 staining. Our results indicate that *B. abortus*-infected LX-2 cells exhibited an increase of TUNEL positive cells, cleaved caspase-3, and apoptotic nuclei as revealed by Hoechst 33342 staining as compared to uninfected controls (Fig. 7), thus indicating a pro-apoptotic effect of *Brucella* infection. Apoptosis depended on the expression of a functional T4SS, since the percentage of apoptotic cells did not differ significantly between LX-2 cells infected with *B. abortus virB* mutant and uninfected

controls. These results indicated that after 48 h post-infection *B. abortus* infection induces apoptosis of LX-2 cells.

PI3-kinase and lysosomal proteases are necessary to induce apoptosis of *B. abortus* infected LX-2 cells

Experiments were conducted to study if PI3-kinase signaling pathway, lysosomal protein degradation and apoptosis are related phenomena during *B. abortus* infection. To determine if this phenomena are necessary to induce apoptosis, infection experiment were performed in the presence of wortmannin and leupeptin plus E64 and the presence of apoptotic cells was determined by TUNEL assay, cleaved caspase-3 expression, and Hoechst 33342 staining. *B. abortus*-infected LX-2 cells exhibited an increase of TUNEL positive cells, cleaved caspase-3, and apoptotic nuclei as revealed by Hoechst 33342 staining as compared to uninfected controls (Fig. 8), Apoptosis was depended on the PI3-kinase signaling pathway and lysosomal protein degradation, since the percentage of apoptotic cells was significantly reduced when infection experiments were performed in the presence of the mentioned inhibitors (Fig. 8). These results indicated that PI3-kinase and lysosomal proteases are necessary to induce apoptosis in *B. abortus* infected hepatic stellate cells.

DISCUSSION

Brucellosis is a worldwide zoonosis characterized by hepatomegaly, splenomegaly and peripheral lymphadenopathy. It is a chronic and debilitating infection caused by Gram-negative facultative intracellular bacteria that infect domestic and wild

321 animals and can be transmitted to humans (2, 5). However, although numerous studies
322 have focused on brucellar liver histopathology (1, 4-6), the pathogenic mechanisms of
323 liver disease caused by *Brucella* have not been completely elucidated.

324 In humans, the liver is frequently affected during active brucellosis. The
325 frequency of liver involvement in active brucellosis ranges from 5% to 52% or more
326 (5). In any circumstance, the persistence of an infectious stimulus might drive liver
327 fibrosis because its presence could induce marked alterations in a variety of immune
328 and structural cells, leading to a healing phenotype which is characterized by the
329 deposition of extracellular matrix (43). This occurs as a compensatory response to the
330 tissue repairing process in a wide range of chronic liver injures. However, although
331 numerous studies have focused on brucellar liver histopathology (4), the pathogenic
332 mechanisms of liver disease caused by *Brucella* have not been completely elucidated.

333 Autophagy is a cellular pathway crucial for development, differentiation,
334 survival, and homeostasis. Its implication in human diseases has been highlighted in the
335 last years (13). In addition several data show that autophagy is involved in major
336 aspects of hepatology (44). In liver, autophagy may supply energy for activation of
337 HSCs and this activation can as well induce some liver diseases including hepatic
338 fibrogenesis (13). Autophagy fuels activation of HSCs inducing type I collagen
339 synthesis, as it was documented during cellular activation both *in vitro* and *in vivo* in
340 mice following either carbon tetrachloride (CCL4) or thioacetamide (TAA)-induced
341 liver injury, as well as in human HSCs from hepatitis B-infected liver (7). Accordingly,
342 our results indicate that upon infection of LX-2 cells, *B. abortus* triggers autophagy
343 activation characterized by the up-regulation of Beclin-1 expression, the increase in
344 LC3 II/LC3 I ratio and the down-modulation of p62. This was at least in part associated
345 with a profibrogenic response characterized by inhibition of MMP-9 secretion,

induction of collagen deposition and TGF-β1 secretion in a way that involved a functional T4SS and its BPE005 effector protein.

As was mentioned, liver fibrosis is the excessive accumulation of extracellular matrix proteins including collagen that occurs in most types of chronic liver diseases. Advanced liver fibrosis results in cirrhosis, liver failure, and portal hypertension. In human brucellosis, it has been reported as a possible causal relationship between *B. abortus* infection and cirrhosis (4); however, the presence of liver cirrhosis is a debatable issue, since in the studies reported, viral hepatitis was not excluded by the authors (5, 45, 46). In addition, cirrhosis was not observed during *Brucella* infection in animal models, indicating that although the ability of *Brucella* to induce a fibrotic phenotype in HSCs, other factors could be involved to reduce the high fibrosis necessary to induce hepatic cirrhosis (17) The reversion of fibrotic phenotype and the concomitant resolution of hepatic fibrosis play an important role in the resolution of the pathogenesis of hepatic fibrosis without induction of cirrhosis. Recent studies suggest that apoptosis becomes the overriding process with resulting net HSCs loss from the liver. This clearance of activated HSCs by apoptosis paved the way for the recovery of hepatic fibrosis (47, 48). Thereby, our results indicate that *B. abortus* was able to induce fibrosis with concomitant autophagy pathway activation in LX-2 cells at 24 h post-infection. However, at 48 h post-infection caspase-mediated cleavage of Beclin-1 inactivates autophagy mediated by Beclin-1 and enhances apoptosis with concomitant apoptosis cell death.

Autophagy and apoptosis are two important and interconnected stress-response mechanisms; and this phenomenon in which autophagy precedes apoptosis could control, at least in part, the liver fibrosis and inhibit the development of cirrhosis. This

370 could partly explain that the development of cirrhosis is rare during hepatic brucellosis
371 (5).

372 Taken together, these results indicate that upon infection of HSCs, *B. abortus*
373 triggers a profibrotic response coinciding with the autophagic pathway activation and
374 then apoptosis cell death of activated HSCs that modulate the fibrotic phenotype.

375

376 **ACKNOWLEDGMENTS**
377

378 We thank Scott Friedman for LX-2 cells and also Horacio Salomón and the staff
379 of the Instituto de Investigaciones Biomédicas en Retrovirus y SIDA (INBIRS) for their
380 assistance with biosafety level 3 laboratory uses. P.C.A.B. A.I.P.V. and C.K.H. are
381 recipients of a fellowship from CONICET. G.H.G., D.J.C., and M.V.D. are members of
382 the Research Career of CONICET. The funding agencies had no role in study design,
383 data collection and analysis, decision to publish, or preparation of the manuscript.

384

385

REFERENCES

1. **Young EJ.** 1989. Clinical manifestations of human brucellosis. Edited by Young EJ and Corbel MJ, Brucellosis: clinical and laboratory aspects, CRC Press. Boca Raton, FL.
2. **Pappas G, Akritidis N, Bosilkovski M, Tsianos E.** 2005. Brucellosis. N Engl J Med **352:**2325-2336.
3. **Colmenero JD, Reguera JM, Martos F, Sanchez-De-Mora D, Delgado M, Causse M, Martin-Farfan A, Juarez C.** 1996. Complications associated with Brucella melitensis infection: a study of 530 cases. Medicine (Baltimore) **75:**195-211.
4. **Akritidis N, Tzivras M, Delladetsima I, Stefanaki S, Moutsopoulos HM, Pappas G.** 2007. The liver in brucellosis. Clin Gastroenterol Hepatol **5:**1109-1112.
5. **Madkour MM.** 2001. Osteoarthicular brucellosis. Edited by Madkour MM, Madkour's brucellosis, 2nd ed. Springer-Verlag, Berlin, Germany.
6. **Young EJ, Hasanjani Roushan MR, Shafae S, Genta RM, Taylor SL.** 2014. Liver histology of acute brucellosis caused by Brucella melitensis. Hum Pathol **45:**2023-2028.
7. **Hernandez-Gea V, Friedman SL.** 2012. Autophagy fuels tissue fibrogenesis. Autophagy **8:**849-850.
8. **Bataller R, Brenner DA.** 2005. Liver fibrosis. J Clin Invest **115:**209-218.
9. **Jeng GW, Wang CR, Liu ST, Su CC, Tsai RT, Yeh TS, Wen CL, Wu YQ, Lin CY, Lee GL, Chen MY, Liu MF, Chuang CY, Chen CY.** 1997. Measurement of synovial tumor necrosis factor-alpha in diagnosing emergency patients with bacterial arthritis. Am J Emerg Med **15:**626-629.
10. **Bissell DM, Wang SS, Jarnagin WR, Roll FJ.** 1995. Cell-specific expression of transforming growth factor-beta in rat liver. Evidence for autocrine regulation of hepatocyte proliferation. J Clin Invest **96:**447-455.
11. **Roux CM, Rolan HG, Santos RL, Beremand PD, Thomas TL, Adams LG, Tsolis RM.** 2007. Brucella requires a functional Type IV secretion system to elicit innate immune responses in mice. Cell Microbiol **9:**1851-1869.
12. **Tahashi Y, Matsuzaki K, Date M, Yoshida K, Furukawa F, Sugano Y, Matsushita M, Himeno Y, Inagaki Y, Inoue K.** 2002. Differential regulation of TGF-beta signal in hepatic stellate cells between acute and chronic rat liver injury. Hepatology **35:**49-61.
13. **Song Y, Zhao Y, Wang F, Tao L, Xiao J, Yang C.** 2014. Autophagy in hepatic fibrosis. Biomed Res Int **2014:**436242.
14. **Mao YQ, Fan XM.** 2015. Autophagy: A new therapeutic target for liver fibrosis. World J Hepatol **7:**1982-1986.
15. **Yin XM, Ding WX, Gao W.** 2008. Autophagy in the liver. Hepatology **47:**1773-1785.
16. **Kiyono K, Suzuki HI, Matsuyama H, Morishita Y, Komuro A, Kano MR, Sugimoto K, Miyazono K.** 2009. Autophagy is activated by TGF-beta and potentiates TGF-beta-mediated growth inhibition in human hepatocellular carcinoma cells. Cancer Res **69:**8844-8852.

17. **Arriola Benitez PC, Rey Serantes D, Herrmann CK, Pesce Viglietti AI, Vanzulli S, Giambartolomei GH, Comerci DJ, Delpino MV.** 2016. The Effector Protein BPE005 from Brucella abortus Induces Collagen Deposition and Matrix Metalloproteinase 9 Downmodulation via Transforming Growth Factor beta1 in Hepatic Stellate Cells. Infect Immun **84:**598-606.
18. **Scian R, Barrionuevo P, Giambartolomei GH, Fossati CA, Baldi PC, Delpino MV.** 2011. Granulocyte-macrophage colony-stimulating factor- and tumor necrosis factor alpha-mediated matrix metalloproteinase production by human osteoblasts and monocytes after infection with Brucella abortus. Infect Immun **79:**192-202.
19. **Mizushima N, Yoshimori T, Levine B.** 2010. Methods in mammalian autophagy research. Cell **140:**313-326.
20. **Scian R, Barrionuevo P, Giambartolomei GH, De Simone EA, Vanzulli SI, Fossati CA, Baldi PC, Delpino MV.** 2011. Potential role of fibroblast-like synoviocytes in joint damage induced by Brucella abortus infection through production and induction of matrix metalloproteinases. Infect Immun **79:**3619-3632.
21. **Hibbs MS, Hasty KA, Seyer JM, Kang AH, Mainardi CL.** 1985. Biochemical and immunological characterization of the secreted forms of human neutrophil gelatinase. J Biol Chem **260:**2493-2500.
22. **Arriola Benitez PC, Scian R, Comerci DJ, Serantes DR, Vanzulli S, Fossati CA, Giambartolomei GH, Delpino MV.** 2013. Brucella abortus induces collagen deposition and MMP-9 down-modulation in hepatic stellate cells via TGF-beta1 production. Am J Pathol **183:**1918-1927.
23. **Thoen LF, Guimaraes EL, Dolle L, Mannaerts I, Najimi M, Sokal E, van Grunsven LA.** 2011. A role for autophagy during hepatic stellate cell activation. J Hepatol **55:**1353-1360.
24. **Shintani T, Klionsky DJ.** 2004. Autophagy in health and disease: a double-edged sword. Science **306:**990-995.
25. **He C, Levine B.** 2010 The Beclin 1 interactome. Curr Opin Cell Biol **22:**140-149.
26. **Lippai M, Low P.** 2014. The role of the selective adaptor p62 and ubiquitin-like proteins in autophagy. Biomed Res Int **2014:**832704.
27. **Border WA, Noble NA.** 1994. Transforming growth factor beta in tissue fibrosis. N Engl J Med **331:**1286-1292.
28. **Sieira R, Comerci DJ, Sanchez DO, Ugalde RA.** 2000. A homologue of an operon required for DNA transfer in Agrobacterium is required in Brucella abortus for virulence and intracellular multiplication. J Bacteriol **182:**4849-4855.
29. **Rolan HG, Tsolis RM.** 2008. Inactivation of the type IV secretion system reduces the Th1 polarization of the immune response to Brucella abortus infection. Infect Immun **76:**3207-3213.
30. **Gomes MT, Campos PC, Oliveira FS, Corsetti PP, Bortoluci KR, Cunha LD, Zamboni DS, Oliveira SC.** 2013. Critical role of ASC inflammasomes and bacterial type IV secretion system in caspase-1 activation and host innate resistance to Brucella abortus infection. J Immunol **190:**3629-3638.
31. **Marchesini MI, Herrmann CK, Salcedo SP, Gorvel JP, Comerci DJ.** 2011. In search of Brucella abortus type IV secretion substrates: screening and

identification of four proteins translocated into host cells through VirB system. Cell Microbiol **13:**1261-1274.

32. **Myeni S, Child R, Ng TW, Kupko JJ, 3rd, Wehrly TD, Porcella SF, Knodler LA, Celli J.** 2013. Brucella modulates secretory trafficking via multiple type IV secretion effector proteins. PLoS Pathog **9:**e1003556.
33. **de Barsy M, Jamet A, Filopon D, Nicolas C, Laloux G, Rual JF, Muller A, Twizere JC, Nkengfac B, Vandenhaute J, Hill DE, Salcedo SP, Gorvel JP, Letesson JJ, De Bolle X.** 2011. Identification of a Brucella spp. secreted effector specifically interacting with human small GTPase Rab2. Cell Microbiol **13:**1044-1058.
34. **de Jong MF, Sun YH, den Hartigh AB, van Dijl JM, Tsolis RM.** 2008. Identification of VceA and VceC, two members of the VjbR regulon that are translocated into macrophages by the Brucella type IV secretion system. Mol Microbiol **70:**1378-1396.
35. **Salcedo SP, Marchesini MI, Lelouard H, Fugier E, Jolly G, Balor S, Muller A, Lapaque N, Demaria O, Alexopoulou L, Comerci DJ, Ugalde RA, Pierre P, Gorvel JP.** 2008. Brucella control of dendritic cell maturation is dependent on the TIR-containing protein Btp1. PLoS Pathog **4:**e21.
36. **de Barsy M, Mirabella A, Letesson JJ, De Bolle X.** 2012. A Brucella abortus cstA mutant is defective for association with endoplasmic reticulum exit sites and displays altered trafficking in HeLa cells. Microbiology **158:**2610-2618.
37. **Radhakrishnan GK, Yu Q, Harms JS, Splitter GA.** 2009. Brucella TIR Domain-containing Protein Mimics Properties of the Toll-like Receptor Adaptor Protein TIRAP. J Biol Chem **284:**9892-9898.
38. **Lacerda TL, Salcedo SP, Gorvel JP.** 2013. Brucella T4SS: the VIP pass inside host cells. Curr Opin Microbiol **16:**45-51.
39. **Dohmer PH, Valguarnera E, Czibener C, Ugalde JE.** 2014. Identification of a type IV secretion substrate of Brucella abortus that participates in the early stages of intracellular survival. Cell Microbiol **16:**396-410.
40. **Hamer I, Goffin E, De Bolle X, Letesson JJ, Jadot M.** 2014. Replication of Brucella abortus and Brucella melitensis in fibroblasts does not require Atg5-dependent macroautophagy. BMC Microbiol **14:**223.
41. **Starr T, Child R, Wehrly TD, Hansen B, Hwang S, Lopez-Otin C, Virgin HW, Celli J.** 2012. Selective subversion of autophagy complexes facilitates completion of the Brucella intracellular cycle. Cell Host Microbe **11:**33-45.
42. **Ryter SW, Mizumura K, Choi AM.** 2014. The impact of autophagy on cell death modalities. Int J Cell Biol **2014:**502676.
43. **Meneghin A, Hogaboam CM.** 2007. Infectious disease, the innate immune response, and fibrosis. J Clin Invest **117:**530-538.
44. **Rautou PE, Mansouri A, Lebrec D, Durand F, Valla D, Moreau R.** 2010. Autophagy in liver diseases. J Hepatol **53:**1123-1134.
45. **Mc CN, Eisele CW.** 1951. Brucella hepatitis leading to cirrhosis of the liver. AMA Arch Intern Med **88:**793-802.
46. **Spink WW.** 1956. Brucellosis; epidemiology, clinical manifestations, diagnosis. Semin Int **5:**15-17.
47. **Kong D, Zhang F, Zhang Z, Lu Y, Zheng S.** 2013. Clearance of activated stellate cells for hepatic fibrosis regression: molecular basis and translational potential. Biomed Pharmacother **67:**246-250.

48. **Elsharkawy AM, Oakley F, Mann DA.** 2005. The role and regulation of hepatic stellate cell apoptosis in reversal of liver fibrosis. Apoptosis **10:**927-939.

534 **FIGURE LEGENDS**

535

536 **Figure 1:** *B. abortus* infection induces autophagy in LX-2 cells. LX-2 cells were
537 infected with *B. abortus* at MOI 100 and 1000 , cell lysates obtained at 24 h
538 postinfection were used to determine LC3 I and II, Beclin-1 and p62 production by
539 Western blotting (A). Densitometric analysis of results from three independent
540 experiments performed as described for panel A; LC3 II/LC3 I ratio (B), Beclin-1 (C)
541 and p62 (D). Data are given as the means ± SD from at least three individual
542 experiments. *P<0.05, **P<0.01 versus noninfected cells (N.I.).

543

544 **Figure 2:** *B. abortus* induction of a fibrotic phenotype depends on PI3-kinase and
545 lysosomal proteases. Effect of wortmannin (wort), and E64 plus leupeptin
546 (E64+leupeptin) in the inhibition of MMP-9 secretion induced by *B. abortus* infection
547 by zymography 24 h postinfection (A). wort and E64+leupeptin effect on the induction
548 of collagen deposition induced by *B. abortus* infection as determined by quantification
549 of Sirius red staining 7 days after infection (B). Effect of wort and E64+leupeptin on
550 TGF-β1 secretion during *B. abortus* infection (C). Effect of rapamycin during *B.*
551 *abortus* infection on MMP-9 secretion by zymography 24 h postinfection (D) and
552 collagen deposition determined by quantification of Sirius red staining 7 days after
553 infection (E). Data are given as the means ± SD from at least three individual
554 experiments. *P<0.05, ***P<0.001 versus infected and untreated cells.

555

556 **Figure 3:** *B. abortus* induces autophagy in LX-2 cells in a VirB-dependent manner. LX-
557 2 cells were infected with *B. abortus* (*Ba*) and its isogenic mutant *virB10* (Δ*virB10*) at
558 MOI 100 and 1000 and cells were stained at 24 h postinfection to determine LC3, and

559 Beclin-1 by immunofluorescense (A). Quantitative analysis of experiments presented in
560 panel A (B, C and D). Data are given as the means ± SD from at least three individual
561 experiments. *P<0.05, **P<0.0, ***P<0.001 versus noninfected cells (N.I.).
562
563 **Figure 4:** VirB-dependent effector protein BPE005 is responsible for the autophagy
564 phenotype. LX-2 cells were infected with *B. abortus* (*Ba*), its isogenic mutant *virB10*
565 (Δ*virB10*), *bpe005* (Δ*bpe005*) and the complemented *bpe005* mutant (c*bpe005*) at MOI
566 1000 and cell lysates obtained at 24 h postinfection were used to determine LC3 I/II by
567 Western blott (A). Densitometric analysis of results from two independent experiments
568 performed as described for panel A (B). Data are given as the means ± SD from at least
569 three individual experiments. ***P<0.001 versus noninfected cells (N.I.); ### P<0.001
570 versus *B. abortus* (Ba).
571
572 **Figure 5:** BPE005 protein induction of a fibrotic phenotype depends on PI3-kinase,
573 lysosomal proteases and autophagosome-lysosome fusion. LX-2 cells were transfected
574 with BPE005 plasmid DNA (pBPE005) or with pcDNA3-c-myc as a control (pCtrl.),
575 and the effect of chloroquine (CQ), bafilomycin (Baf.), wortmannin (wort), and E64
576 plus leupeptin (E64+leupeptin) in the inhibition of MMP-9 secretion was determined by
577 zymography at 24 h after transfection (A). CQ, Baf., wort. and E64+leupeptin effect on
578 the induction of collagen deposition was determined by quantification of Sirius red
579 staining 7 days after transfection (B). Data are given as the means ± SD from at least
580 three individual experiments. ***P<0.001 versus transfected and untreated cells.
581
582 **Figure 6:** *B. abortus* infection induces cleavage of Beclin-1. LX-2 cells were infected
583 with *B. abortus* at MOI 100 and 1000 and cell lysates obtained at 48 h postinfection

were used to determine LC3 I and II, Beclin-1 and p62 production by Western blotting (A). Densitometric analysis of results from two independent experiments performed as described for panel A; LC3 II/LC3 I ratio (B), Beclin-1 (C), Cleaved Beclin-1 (D) and p62 (E). Data are given as the means ± SD from at least three individual experiments. *P<0.05, **p<0.01, versus noninfected cells (N.I.).

Figure 7: *B. abortus* infection induces apoptosis of LX-2 cells. LX-2 cells were infected with *B. abortus* (*Ba*) and its isogenic mutant *virB10* (Δ*virB10*) at MOI 100 and 1000; and apoptosis was evaluated at 48 h postinfection by TUNEL, caspase-3 and Hoechst staining by fluorescence microscopy (A). Quantitative analysis of experiments presented in panel A; TUNEL (B), cleaved caspase-3 (C) and Hoechst 33342 (D). Data are given as the means ± SD from at least three individual experiments. .*P < 0.05, **p<0.01, ***P<0.001 versus noninfected cells (N.I.).

Figure 8: *B. abortus* infection induces apoptosis of LX-2 cells that is dependent on PI3-kinase and lysosomal proteases. Effect of wortmannin (wort,), and E64 plus leupeptin (E64+leupeptin) in the apoptosis induced by *B. abortus* infection at 48 h postinfection. The presence of apoptotic cells were determined and quantified by TUNEL assay (A), cleaved caspase-3 expression (B), and Hoechst 33342 staining (C). Data are given as the means ± SD from at least three individual experiments. .*P < 0.05, **p<0.01, ***P<0.001 versus infected and untreated cells.

Figure 1

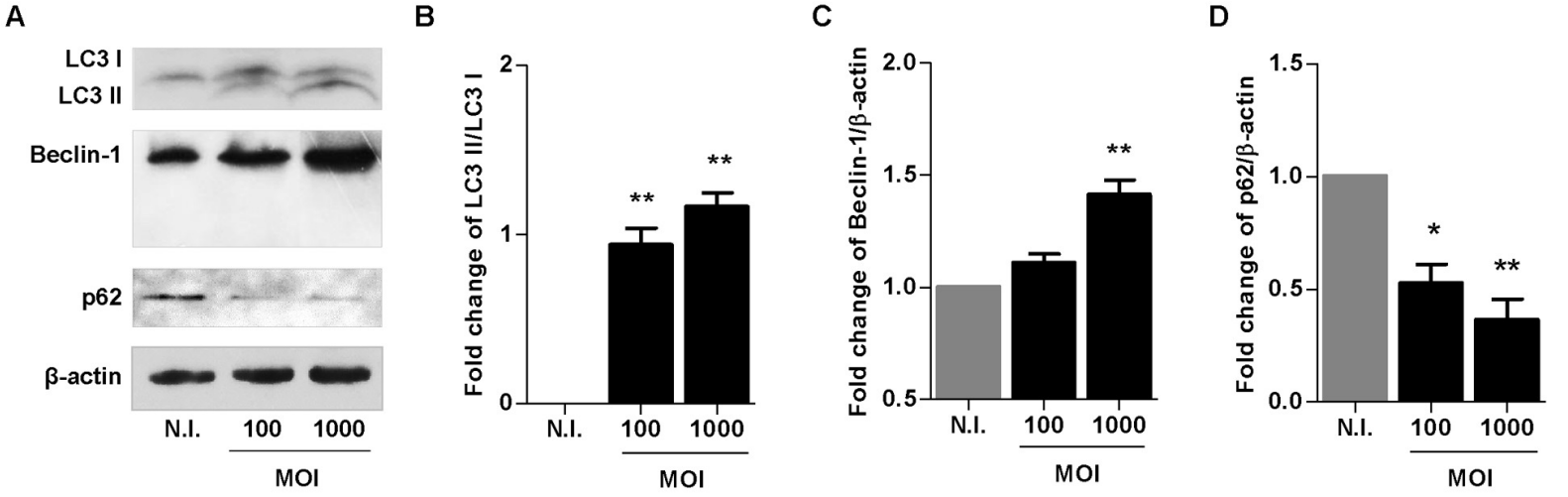
A
LC3 I
LC3 II
Beclin-1
p62
β-actin
N.I.
100
1000
MOI
B
Fold change of LC3 II/LC3 I
2
1
0
**
**
N.I.
100
1000
MOI
C
Fold change of Beclin-1/β-actin
2.0
1.5
1.0
0.5
**
N.I.
100
1000
MOI
D
Fold change of p62/β-actin
1.5
1.0
0.5
0.0
*
**
N.I.
100
1000
MOI

Figure 2

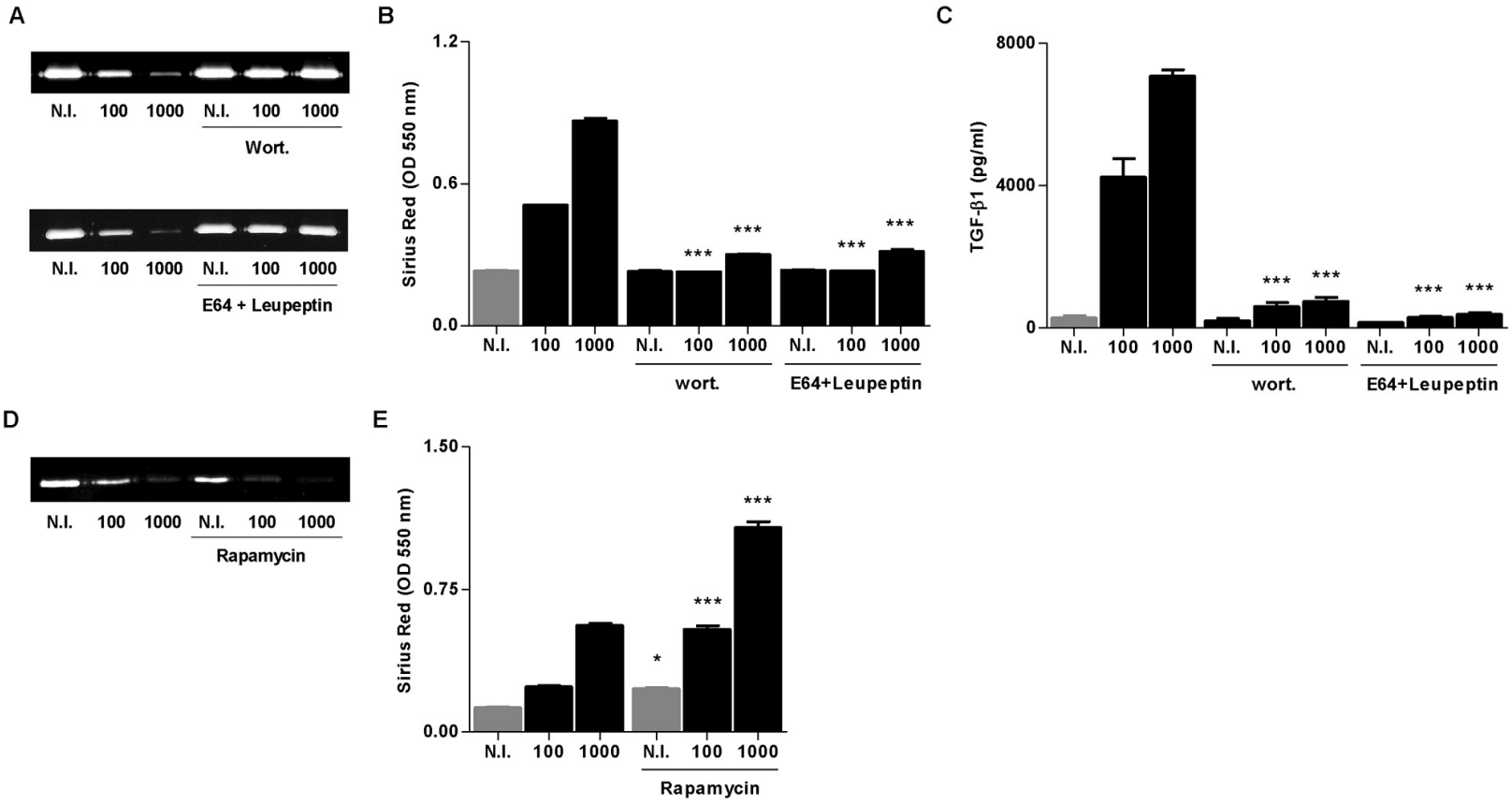
A
N.I. 100 1000 N.I. 100 1000
Wort.
N.I. 100 1000 N.I. 100 1000
E64 + Leupeptin
B
Sirius Red (OD 550 nm)
1.2
0.6
0.0
N.I. 100 1000 N.I. 100 1000 N.I. 100 1000
wort.
E64+Leupeptin
C
TGF-β1 (pg/ml)
8000
4000
0
N.I. 100 1000 N.I. 100 1000 N.I. 100 1000
wort.
E64+Leupeptin
D
N.I. 100 1000 N.I. 100 1000
Rapamycin
E
Sirius Red (OD 550 nm)
1.50
0.75
0.00
N.I. 100 1000 N.I. 100 1000
Rapamycin

Figure 3

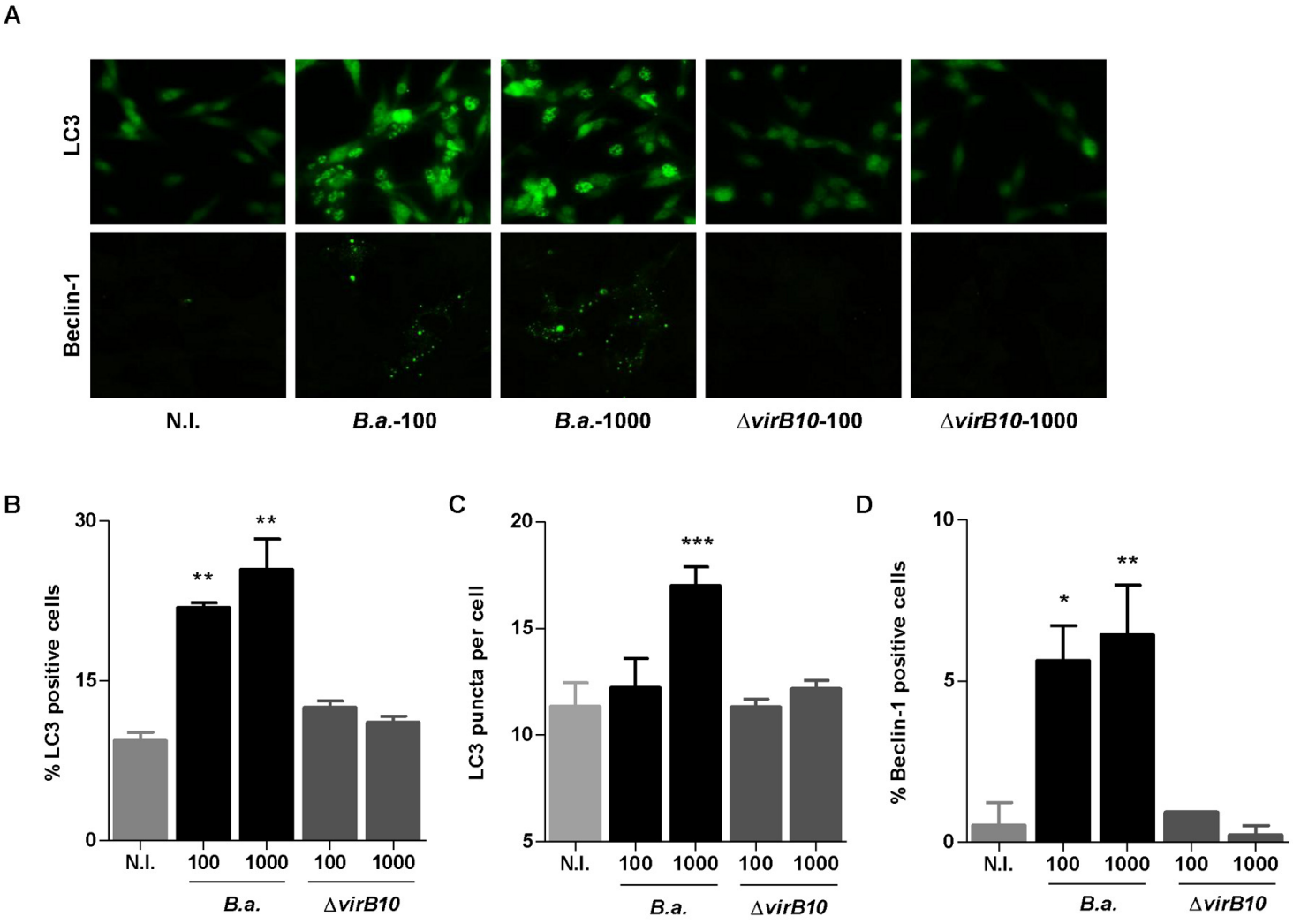
A
LC3
Beclin-1
N.I.
B.a.-100
B.a.-1000
ΔvirB10-100
ΔvirB10-1000
B
% LC3 positive cells
30
15
0
**
**
N.I.
100
1000
100
1000
B.a.
ΔvirB10
C
LC3 puncta per cell
20
15
10
5
***
N.I.
100
1000
100
1000
B.a.
ΔvirB10
D
% Beclin-1 positive cells
10
5
0
*
**
N.I.
100
1000
100
1000
B.a.
ΔvirB10

Figure 4

A

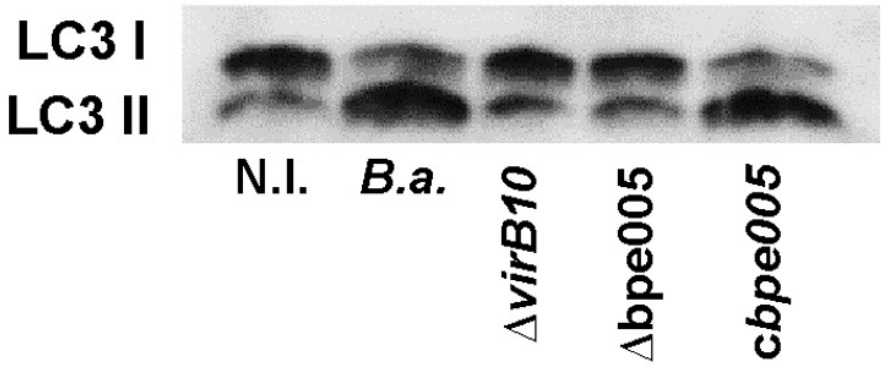
LC3 I
LC3 II
N.I.
B.a.
ΔvirB10
Δbpe005
cbpe005

B

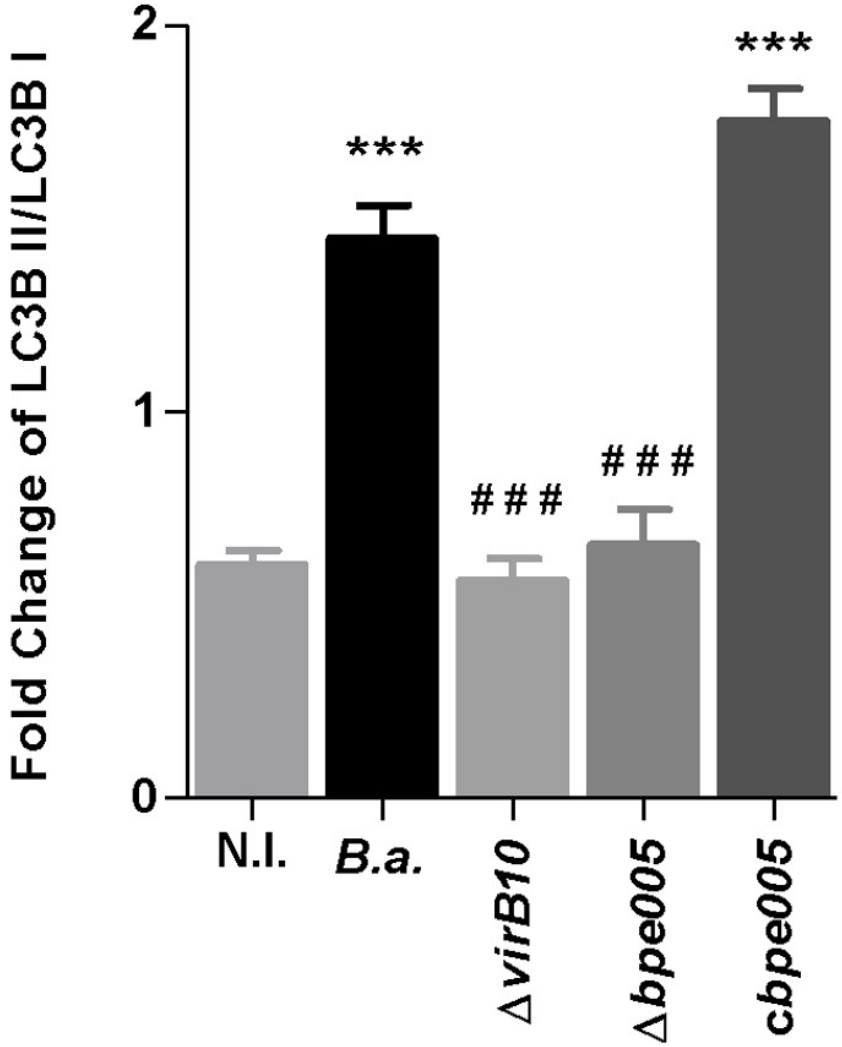
Fold Change of LC3B II/LC3B I
2
1
0
***
***
###
###
N.I.
B.a.
ΔvirB10
Δbpe005
cbpe005

Figure 5

A

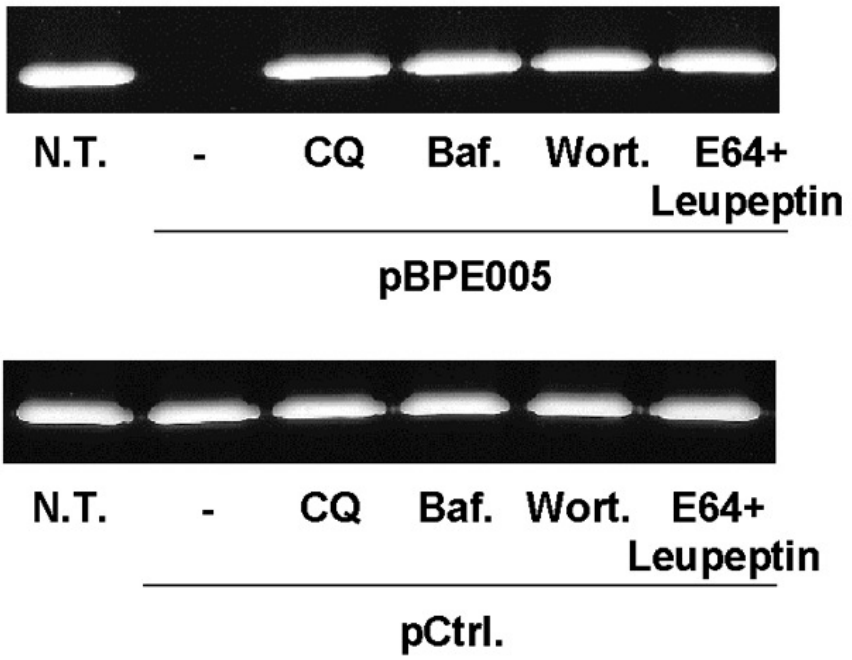
N.T.
-
CQ
Baf.
Wort.
E64+
Leupeptin
pBPE005
N.T.
-
CQ
Baf.
Wort.
E64+
Leupeptin
pCtrl.

B

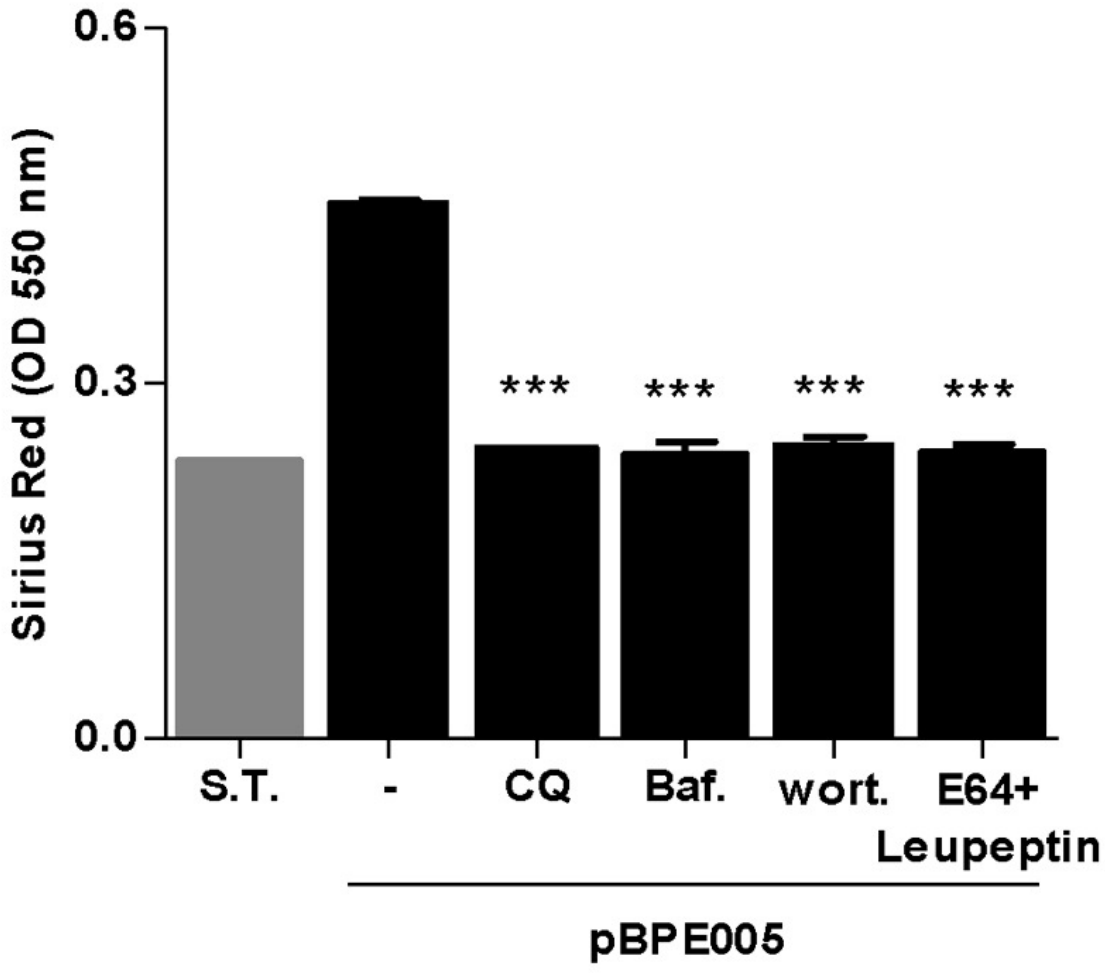
Sirius Red (OD 550 nm)
0.6
0.3
0.0
***
***
***
***
S.T.
-
CQ
Baf.
wort.
E64+
Leupeptin
pBPE005

Figure 6

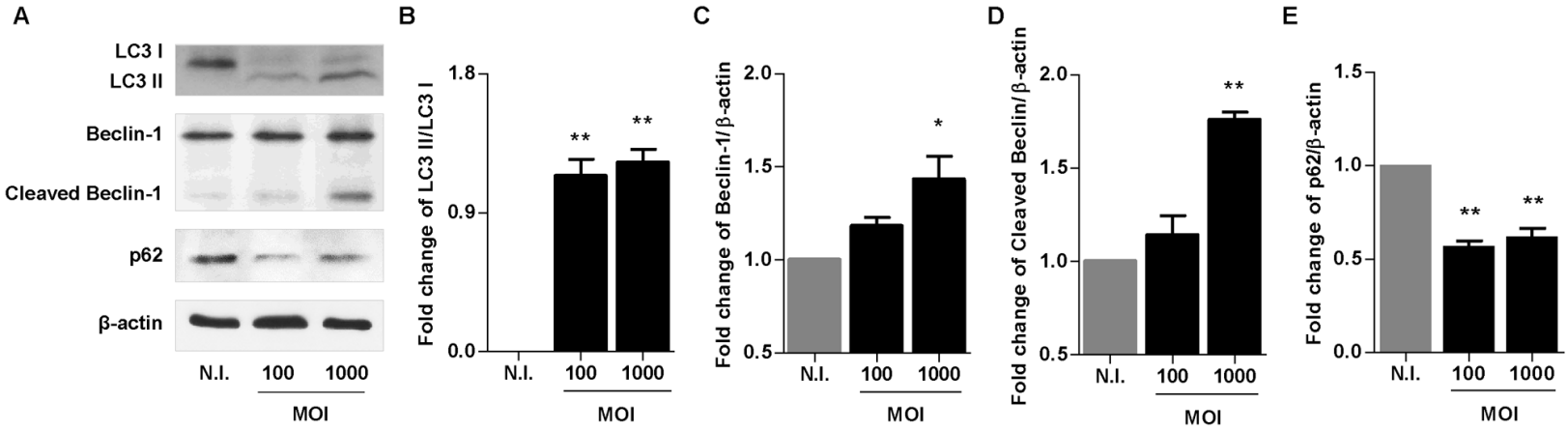
A
LC3 I
LC3 II
Beclin-1
Cleaved Beclin-1
p62
β-actin
N.I.
100
1000
MOI
B
Fold change of LC3 II/LC3 I
1.8
0.9
0.0
**
**
N.I.
100
1000
MOI
C
Fold change of Beclin-1/β-actin
2.0
1.5
1.0
0.5
*
N.I.
100
1000
MOI
D
Fold change of Cleaved Beclin/β-actin
2.0
1.5
1.0
0.5
**
N.I.
100
1000
MOI
E
Fold change of p62/β-actin
1.5
1.0
0.5
0.0
**
**
N.I.
100
1000
MOI

Figure 7

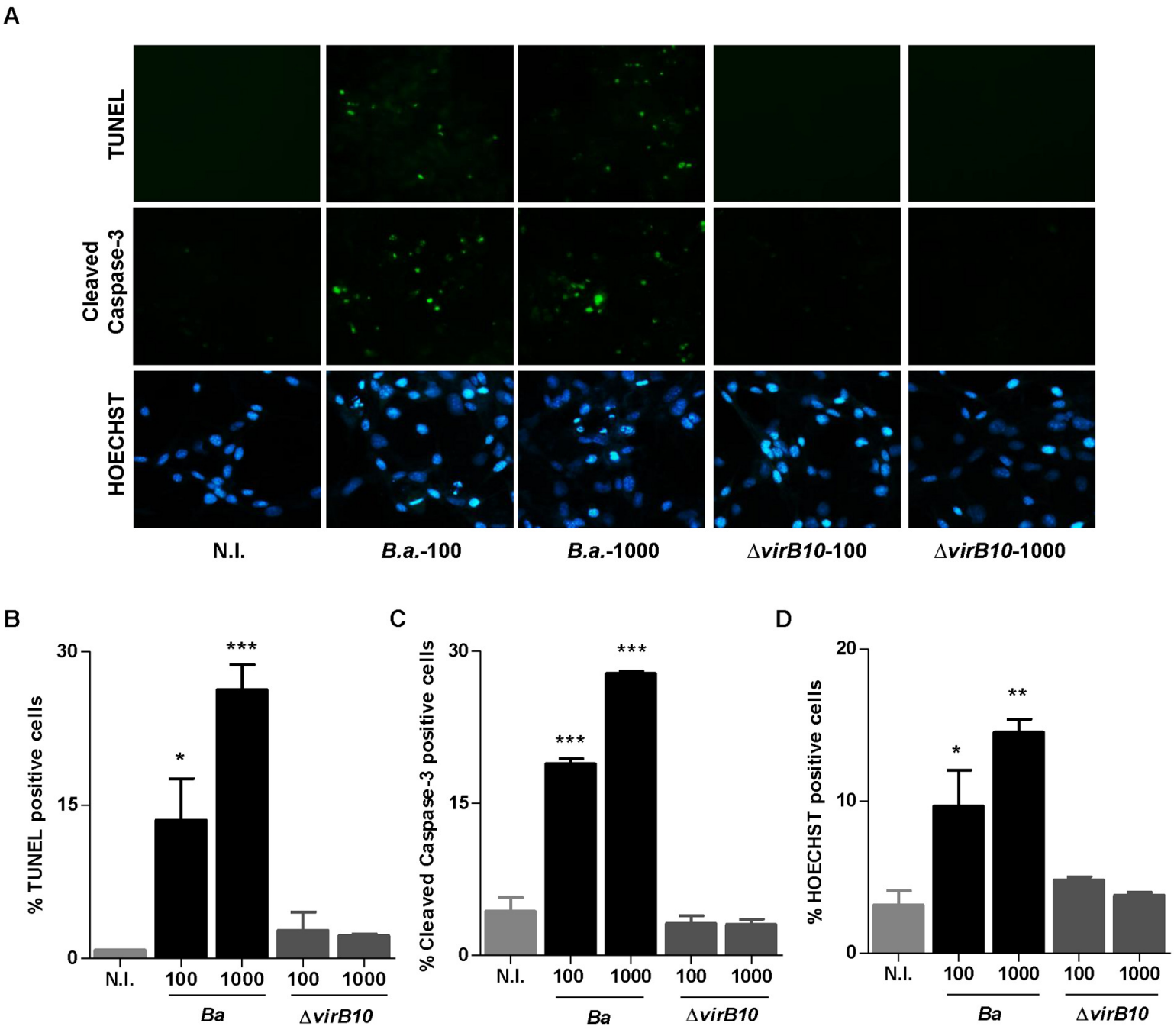
A
TUNEL
Cleaved Caspase-3
HOECHST
N.I.
B.a.-100
B.a.-1000
ΔvirB10-100
ΔvirB10-1000
B
% TUNEL positive cells
30
15
0
*
***
N.I.
100
1000
100
1000
Ba
ΔvirB10
C
% Cleaved Caspase-3 positive cells
30
15
0
***
***
N.I.
100
1000
100
1000
Ba
ΔvirB10
D
% HOECHST positive cells
20
10
0
*
**
N.I.
100
1000
100
1000
Ba
ΔvirB10

Figure 8

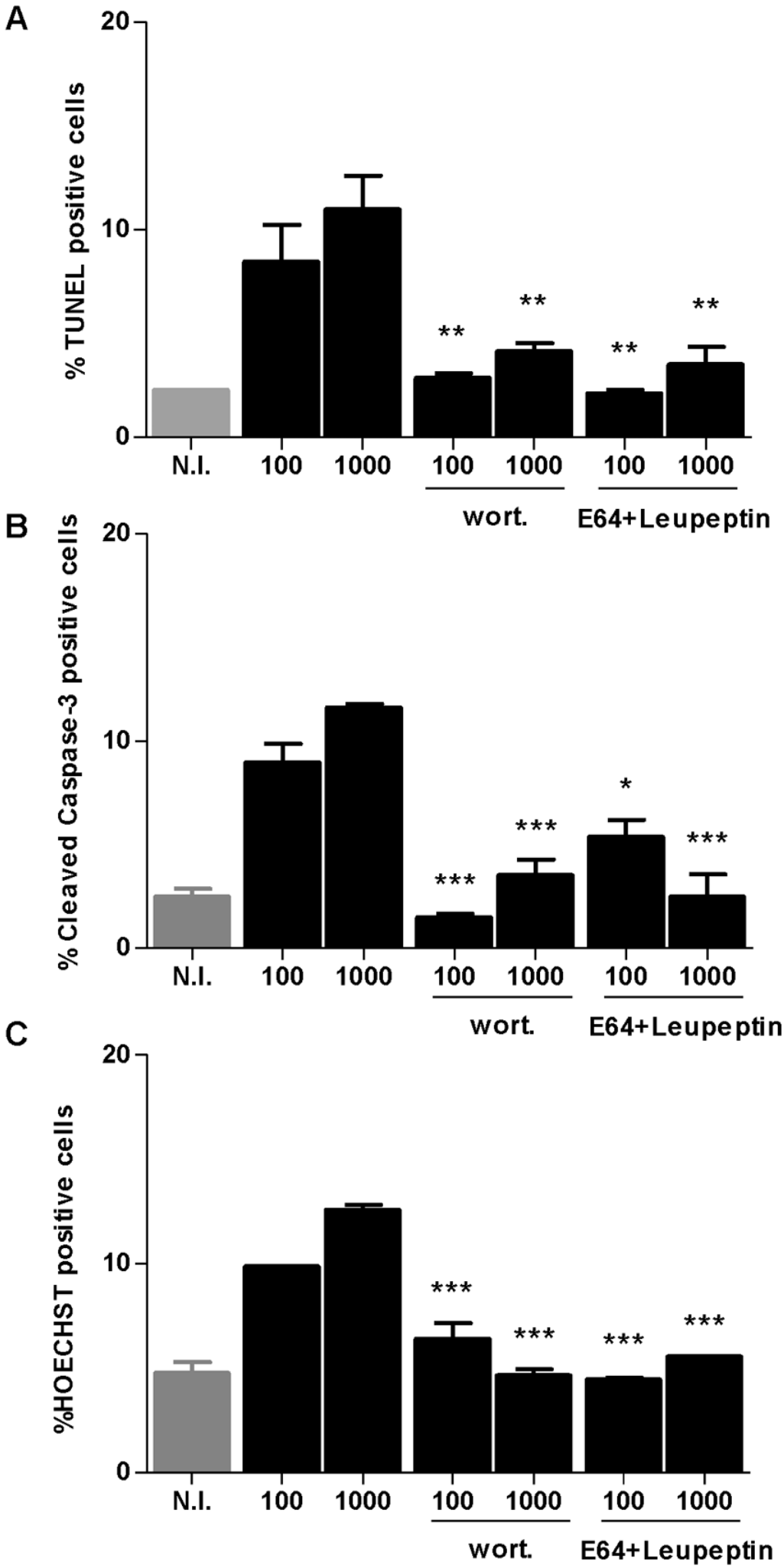
A
20
10
0
% TUNEL positive cells
**
**
**
**
N.I.
100
1000
100
1000
100
1000
wort.
E64+Leupeptin
B
20
10
0
% Cleaved Caspase-3 positive cells
***
***
*
***
N.I.
100
1000
100
1000
100
1000
wort.
E64+Leupeptin
C
20
10
0
%HOECHST positive cells
***
***
***
***
N.I.
100
1000
100
1000
100
1000
wort.
E64+Leupeptin